Proc. Natl. Acad. Sci. USA
Vol. 76, No. 11, pp. 5636–5640, November 1979
Biophysics

Chromophore organization in photosynthetic reaction centers: High-resolution magnetophotoselection

(chlorophyll/bacteriochlorophyll/dye laser/electron spin resonance/triplet)

STEVEN G. BOXER AND MARK G. ROELOFS

Department of Chemistry, Stanford University, Stanford, California 94305

Communicated by Harden M. McConnell, July 2, 1979

ABSTRACT **The electron spin resonance spectrum of the triplet excited state of *Rhodopseudomonas spheroides* R-26 reaction centers has been studied after excitation with the polarized narrow-bandwidth output of a tunable dye laser from 520 to 670 nm. A theory is developed relating experimental observables to the angles between the electronic transition dipole moment of the excited chromophore and the principle magnetic axis system of the triplet state of the dimeric trap. Data is presented which demonstrates that the treatment is correct and useful, and angles are obtained for the Q_x transitions of bacteriopheophytin. High-resolution magnetophotoselection data in the region of the bacteriochlorophyll Q_x transitions can be combined with polarized photobleaching experiments to provide direct information on the structure of dimeric trap.**

Current research on the mechanism of the initial steps in photosynthesis focuses on three problems: (*i*) the identity and stoichiometry of obligatory components, (*ii*) the time sequence of energy and electron transfers and the identity of molecular constituents participating in these transfers, and (*iii*) the spacial relationships among the principle components (relative orientations and distances). For the most widely studied case of the purple photosynthetic bacterium *Rhodopseudomonas spheroides* (R-26 mutant), a great deal of progress has been made in each of these areas as a consequence of the isolation of highly purified, low molecular weight, functional reaction centers (1). These reaction centers contain three small proteins, four bacteriochlorophylls a (BChls), and two bacteriopheophytins a (BPheos, BChl in which 2 H replace Mg) (2). The electronic states of two BChls interact to produce a low-energy trap [$(BChl)_2$ or P870] (3, 4) which, on direct excitation or energy transfer from any other chromophore (5), transfers an electron very rapidly (<6 ps) to a BPheo (6–9). If secondary electron transfer is blocked by prior reduction, the radical ion pair [$(BChl)_2^{+\cdot}$ $BPheo^{-\cdot}$] lives for several nanoseconds before annihilation to neutrals. This process may generate neutrals either in the singlet ground state or the lowest triplet state of $(BChl)_2$ (10). At low temperature the latter pathway predominates (11) and a spin-polarized electron spin resonance (ESR) spectrum characteristic of the $\Delta m_s = \pm 1$ transitions of a triplet species is readily detected and has been discussed (12–14).

Much less is known about reaction center structure. Very recently a number of investigators, notably Clayton *et al.* (15), Rafferty and Clayton (16–18), Vermeglio *et al.* (19), and Shuvalov and Asadov (20), have reported photoselection and linear and circular dichroism measurements on reaction centers, in many cases oriented in stretched films. An analysis of the data provides a detailed picture of the angles among the transition dipole moment axes of each of the reaction center chromophores. At the same time we have adopted an alternate approach which combines high resolution polarized laser excitation and the properties of the triplet ESR signal in order to specify the orientation of the chromophore transition dipole moments in an internal Cartesian axis system. This approach was suggested by earlier qualitative studies of *in vitro* chlorophyll and chromatophore triplets (21, 22). The purpose of this paper is to present the principle and theory of the experiment, a test of its validity and scope, and results for the second excited states of reaction center chromophores.

Principle of experiment and theory

The electronic absorption spectrum of R-26 reaction centers is shown in Fig. 1. Each monomeric chromophore gives rise to two transitions in the 500- to 900-nm region denoted Q_x and Q_y for the higher and lower energy states, respectively (23). There is very good evidence that excitation of *any* transition in the reaction center leads to charge separation with essentially constant quantum yield, after rapid energy transfer to the trap (5, 9). As a consequence, the quantum yield for triplet state formation after annihilation is also independent of the excitation wavelength.

The well-known triplet state ESR spectrum from reaction centers is shown in Fig. 2. In general, peaks in the first derivative presentation of the ESR spectrum of a randomly oriented collection of triplet states originate only from those molecular orientations, the canonical orientations, for which one of the magnetic axes (the principle axis system of the zero-field splitting tensor) coincides with the direction of the external magnetic field (24, 25). Molecules at other orientations give rise to a broad background signal, so the observed spectrum arises from a magnetoselected subpopulation of excited molecules. We assume that this also applies to reaction center triplets, though the spectrum reflects an extreme deviation from a Boltzmann equilibrium population distribution, which in principle could alter the expected peak positions (26).

One can further photoselect a subset of reaction centers by exciting with linearly polarized light. For the special case of direct trap excitation this is the conventional magnetophotoselection technique (27–31). When other chromophores are selectively excited and transfer their energy to the trap, the signal intensity of each peak in the triplet spectrum can be used to determine the component of the sensitizer transition dipole moment vector along each of the trap magnetic axes.

Referring to Fig. 3, the desired angles between the transition dipole moment $\vec{U}$ of the sensitizer and the ith magnetic axis of the trap are ϕ_i, $i = 1, 2$, and 3. The contribution $I_i(\gamma,\theta)$ to the intensity of the signal associated with the ith canonical orientation from those molecules with a given γ is proportional to the number of reaction centers having that γ which absorb light:

$$I_i(\gamma,\theta) = K_i \frac{(\vec{E}\cdot\vec{U})^2}{(|\vec{E}|\,|\vec{U}|)^2} = K_i \cos^2\alpha \qquad [1]$$

The publication costs of this article were defrayed in part by page charge payment. This article must therefore be hereby marked "*advertisement*" in accordance with 18 U. S. C. §1734 solely to indicate this fact.

Abbreviations: BChl, bacteriochlorophyll a; BPheo, bacteriopheophytin a; $(BChl)_2$, *in vivo* BChl special pair; ESR, electron spin resonance.

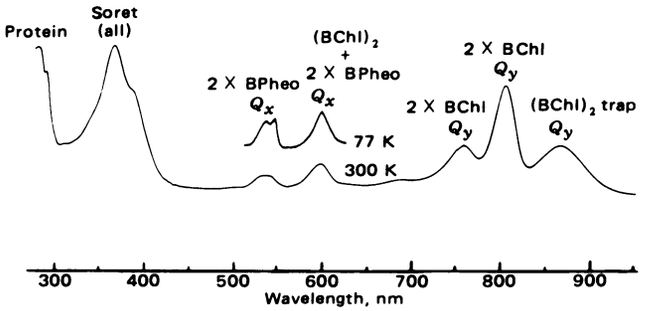

FIG. 1. Electronic absorption spectrum of R-26 reaction centers.

where α is the angle between $\vec{E}$ and $\vec{U}$ and K_i is a constant that accounts for light intensity ($|\vec{E}|^2$), extinction coefficient ($|\vec{U}|^2$), line shape, and instrumental factors. Provided the ith magnetic axis is parallel to $\vec{H}_0$, any rotation of the reaction center about Z yields a canonical orientation, and the total intensity is given by integrating Eq. **1** over all γ:

$$I_i(\theta) = \frac{K_i}{2\pi}\int_0^{2\pi} \cos^2\alpha \, d\gamma.$$

Substituting $\cos\alpha = \sin\theta\sin\phi_i\cos\gamma + \cos\theta\cos\phi_i$ and defining the components along each axis i as $r_i = \cos^2\phi_i$, we obtain:

$$I_i(\theta) = \frac{K_i}{2}[1 - r_i + (3r_i - 1)\cos^2\theta]. \qquad [2a]$$

This treatment assumes negligible depopulation of the ground state (31) and no dependence of triplet yield or spin polarization on γ. According to Eq. **2a** the angular dependence of I_i is predicted to be $\sin^2\theta$, $\cos^2\theta$, or a straight line as r_i is less than, greater than, or equal to $\frac{1}{3}$ (this corresponds to angles θ of less than, greater than, or equal to the magic angle, 54.7°).

It is necessary to account for the effects of depolarized excitation due to scattering or imperfect optics, as discussed by Siegel and Judeikis (30, 31). The constant k is defined as the ratio of the integrated intensity of the depolarized light to that of the polarized light. If $\vec{E}$ is now given spherical coordinates $|\vec{E}|$, β, and θ', depolarized light consists of a random distribution of values for these angles and leads to the following contribution

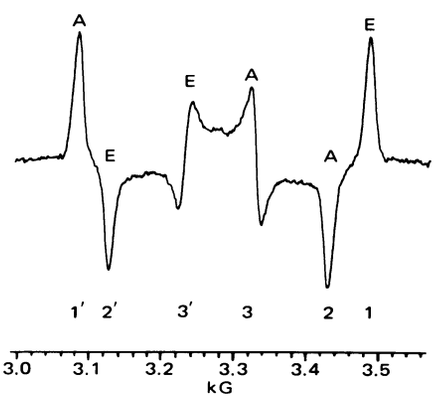

FIG. 2. ESR spectrum of the triplet state of reduced R-26 reaction centers at 80–90 K, excited with depolarized light (λ = 400–700 nm); 1 G = 10^{-4} T. E and A denote emission and absorption signals, respectively.

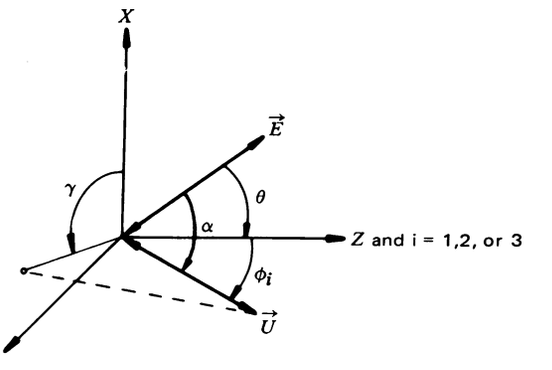

FIG. 3. Axis system for sensitized magnetophotoselection experiment giving angles among the laboratory-fixed axes X, Y, and Z, magnetic field $\vec{H}_0(\vec{H}_0 \| Z)$, electronic transition dipole moment $\vec{U}$, electric field vector of polarized exciting light $\vec{E}$, and principle magnetic axes, i = 1, 2, and 3 of the triplet. $\vec{E}$ lies in the XZ plane and makes an angle θ with $\vec{H}_0$. When a signal arising from the ith (i = 1, 2, and 3) canonical orientation is observed, i is parallel to $\vec{H}_0$. $\vec{U}$ then has spherical coordinates $|\vec{U}|$, γ, and ϕ_i in the laboratory frame.

to the signal intensity due to depolarized (depol) light:

$$I_i^{\text{depol}} = \frac{K_i}{2\pi}\int_0^{2\pi}\frac{1}{2\pi}\int_0^{2\pi}\frac{1}{2}\int_0^{\pi} k\cos^2\alpha\sin\theta' \, d\theta' \, d\beta \, d\gamma$$

$$I_i^{\text{depol}} = K_i\frac{1}{3}k. \qquad [2b]$$

For the convenient special cases of light parallel or perpendicular to $\vec{H}_0$ the sum of Eqs. **2a** and **2b** reduces to:

$$I_i(\|) = K_i\left(r_i + \frac{1}{3}k\right)$$

$$I_i(\perp) = K_i\left(\frac{1}{2} - \frac{1}{2}r_i + \frac{1}{3}k\right), \qquad [3]$$

and the components $\{r_i\}$ can be obtained directly from the polarization ratios:

$$P_i \equiv \frac{I_i(\|) - I_i(\perp)}{I_i(\|) + I_i(\perp)} = \frac{3r_i - 1}{r_i + \frac{4}{3}k + 1}$$

$$r_i = \frac{1 + \left(1 + \frac{4}{3}k\right)P_i}{3 - P_i}. \qquad [4]$$

The experiment consists of measuring $I_i(\|)$ and $I_i(\perp)$ for i = 1, 2, and 3. The desired ϕ_i are obtained by calculating P_i and r_i and substituting into $\phi_i = \cos^{-1}(\pm r_i^{1/2})$.

Given the number of expected transitions (see Fig. 1) we anticipate overlapping absorption bands. Suppose light of wavelength λ is absorbed by two or more transitions (indexed by j) with extinction coefficients $\epsilon_j(\lambda)$ and components $r_{i,j}$ along the ith magnetic axis. Because the triplet quantum yield is independent of which chromophore is excited, the contributions to the signal intensities for θ = 0° and 90° are, using Eqs. **3**:

$$I_i(\|,\lambda) = K_i'\sum_j \epsilon_j(\lambda)\left(r_{i,j} + \frac{1}{3}k\right) \quad \text{and}$$

$$I_i(\perp,\lambda) = K_i'\sum_j \epsilon_j(\lambda)\left(\frac{1}{2} - \frac{1}{2}r_{i,j} + \frac{1}{3}k\right), \qquad [5]$$

where K_i' is a constant involving only light intensity, line shape,

and instrumental factors. Substitution of Eqs. 5 into Eq. 4 gives the polarization ratios as:

$$P_i(\lambda) = \frac{3\bar{r}_i(\lambda) - 1}{\bar{r}_i(\lambda) + \frac{4}{3}k + 1}, \quad [6]$$

where $\bar{r}_i(\lambda)$ is the extinction-weighted average component given by:

$$\bar{r}_i(\lambda) = \frac{\sum_j \epsilon_j(\lambda) r_{i,j}}{\sum_j \epsilon_j(\lambda)}. \quad [7]$$

Experimental

Reaction centers from the R-26 mutant of *R. spheroides* were isolated and analyzed by standard methods, reduced with excess sodium dithionite at room temperature under argon, diluted with 2 vol of glycerol to a final concentration of 0.2 mM, outgassed to a pressure of 1 mtorr, and sealed in quartz tubes. Light-modulated ESR signals were generated in an *X*-band spectrometer using 100-kHz, 20-G field modulation and 10-mW microwave power at 80–90 K. The exciting light was chopped (laser) or square-wave modulated (xenon lamp) at a fixed frequency in the range of 100–500 Hz, and the signal was phase-sensitive detected at the chopping frequency by using a lock-in amplifier and digitized in a Nicolet 1180 computer.

The polarization ratios of peaks 1, 1′, 2, and 2′ were obtained with the field set at the center of the peak while the signal was averaged over 10–20 time constants of the lock-in for light parallel and perpendicular to the field and no light. To obtain P_3 and $P_{3'}$ (see Fig. 2), the magnetic field was swept repetitively through transitions 3 and 3′ for $\theta = 0°$ or 90°, and the signal intensity was taken as the absolute value of the average peak-to-peak voltage of the first derivative line-shape. The ratio of signal intensity to root mean square noise was typically 20:1. An estimate of the standard deviation in P_i was made by repeating the determinations three or four times with different samples at more than half the excitation wavelengths. Implicit in this approach to the determination of the P_i from the measured intensities is the assumption that the signal intensities at the peak positions labeled in Fig. 2 measure exclusively the number of molecules at each canonical orientation in the triplet state [this approximation has been widely applied and tested in conventional magnetophotoselection studies (27–29)]. Alternatively, one could attempt to fit the intensities measured at the peaks to a theoretically generated spectrum.†

Excitation light between 520 and 670 nm was provided by a Coherent 590 CW dye laser pumped by an Ar-ion laser. The bandwidth was less than 0.2 nm and usable ESR signals could be obtained for powers between 25 and 400 mW. The linearly polarized output can be rotated to any angle θ with a $\lambda/2$ double Fresnel rhomb with an accuracy of 2°. Excitation light of wavelength >850 nm was produced by filtering the output of a 300-W xenon lamp successively through 10 cm of water, an 850-nm-long pass filter (Hoya IR 85), and Polaroid HR polarizing film. The following method was used to determine k: the 0-0 band of the $^1L_\alpha$ state of tetracene dissolved in 2-methyltetrahydrofuran was excited at 476.5 nm with 100 mW from the ion laser. This transition is 100% in-plane polarized (33); thus r_1 should be zero ($P_1 = -1$ if $k = 0$), because magnetic axis 1 (the z axis) in the triplet state is perpendicular to the plane. The measured P_1 (−0.80) corresponds to $k = 0.19$.

† We are indebted to K. Sauer, J. Bolt, and R. Friesner for helpful discussions on this point (32).

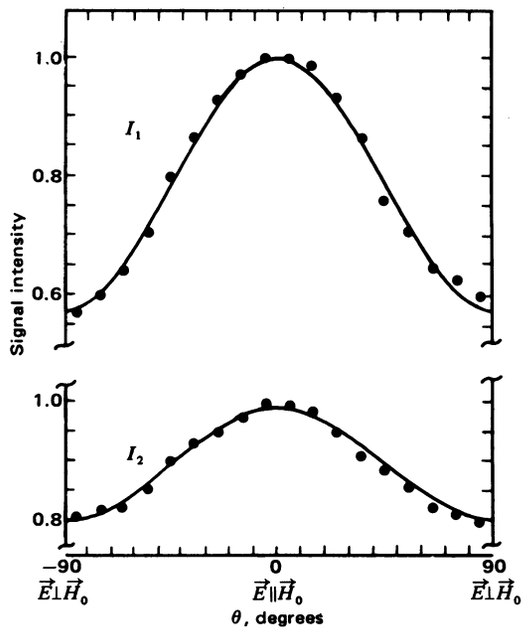

FIG. 4. Signal intensity of peaks 1 and 2 as a function of θ for excitation at 535 nm. Experimental intensities (●) are normalized so that $I_i(0°) = 1.00$. Curves are plots of the sum of Eqs. **2a** and **2b** with $r_1 = 0.49$, $r_2 = 0.39$, $K_1 = 1.80$, $K_2 = 2.18$, and $k = 0.19$.

Results and discussion

As a test of the validity of the approach and theory outlined above, the intensities of a number of peaks in reaction centers were measured as a function of θ at several excitation wavelengths. An example is shown in Fig. 4 for excitation at 535 nm (BPheo region) in which the curves are a plot of Eq. 2 for the specified values of K_i and r_i. Agreement with Eq. 2 is excellent and supports the theoretical treatment outlined above. Fig. 5 shows field swept difference spectra $[I(\parallel)-I(\perp)]$ for several excitation wavelengths in the region of the 600-nm band. It is immediately apparent that narrow bandwidth excitation achieves resolution of at least three absorption bands in this region (compare Fig. 1) and that the angles between each transition moment and the trap axes are very different.

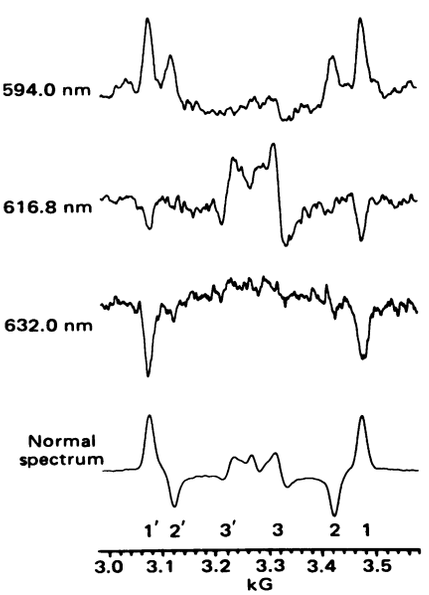

FIG. 5. Field-swept difference triplet ESR spectra $[I(\parallel)-I(\perp)]$ for excitation at the indicated wavelengths, illustrating resolution of differently oriented sensitizer transition dipole moments in the region of the 600-nm absorption band.

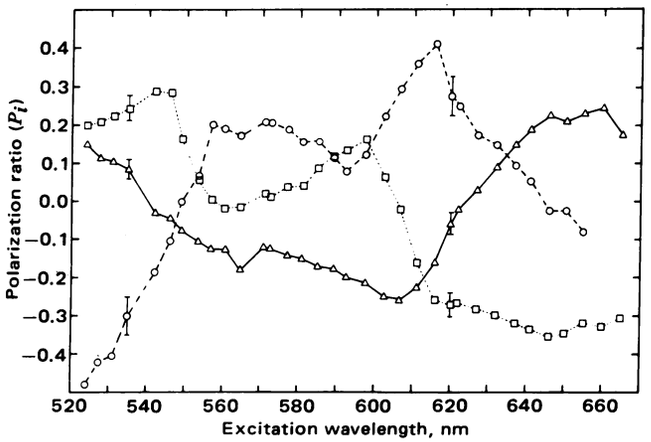

FIG. 6. Polarization ratios $P_1(\lambda)$ (□), $P_2(\lambda)$ (△), and $P_3(\lambda)$ (○). Error bars are 90% confidence intervals based on the variance in P_i.

Fig. 6 shows the polarization ratios at approximately 4-nm intervals in the 520- to 655-nm region. It is clear that there are very large changes in the values of polarization ratios in the neighborhood of the two absorption bands: two overlapping bands are suggested in the BPheo Q_x region around 540 nm, and at least three overlapping bands are found in the BChl Q_x region around 600 nm. According to Eq. 6 it should be possible to deconvolute each of these bands, but we have not attempted to do so at this time, pending the outcome of complete experiments in the 760-, 800-, and 870-nm regions.

A number of semiquantitative comments can be made at this time. Using the assumption that the ith peak arises exclusively from molecules with magnetic axis i parallel to $\vec{H}_0$, $r_{i,j}$ is the square of the ith direction cosine of $\vec{U}_j$ in the Cartesian principle axis system of the zero-field splitting tensor. Then:

$$\sum_i r_{i,j} = 1,$$

and substitution into Eq. 7 gives:

$$\sum_i \bar{r}_i(\lambda) = 1. \qquad [8]$$

That is, the sum over i of experimentally determined components will still be unity even when more than one transition is excited at a given wavelength. Using the data from Fig. 6, the root mean square deviation of $\sum r_i(\lambda)$ from unity was 0.04, which can be interpreted either as a confirmation of Eq. 8 to within ≈4% or as an independent check for the accuracy of the data. In order to calculate meaningful angles in a Cartesian axis system, Eq. 8 must be satisfied. This is accomplished by adding the same correction, $\delta(\lambda)$, to each P_i such that the $r_i(\lambda)$ calculated from them obey Eq. 8:

$$P_i^{\text{corr}}(\lambda) = P_i^{\text{uncorr}}(\lambda) + \delta(\lambda) \quad i = 1, 2, 3 \qquad [9]$$

$$\delta(\lambda) = \frac{1 - \sum_i r_i^{\text{uncorr}}(\lambda)}{4(1+k)\sum_i [3 - P_i^{\text{uncorr}}(\lambda)]^{-2}}, \qquad [10]$$

where r_i^{uncorr} is calculated, using Eq. 4, from the P_i^{uncorr} shown in Fig. 6. The expression for $\delta(\lambda)$ is derived from an analysis to first order of propagation of error in Eq. 4. None of the angles discussed below or given in Table 1 changed by more than 2° when P_i^{corr} was used in place of P_i^{uncorr}.

For both the BPheo and BChl Q_x regions where polarization ratios change strongly with wavelength, the changes occur over a wider range than expected from the absorption spectrum (compare Fig. 1). This is not surprising because the true ratio characteristic of the individual bands will not be observed except for pure absorption by each species. This is best approximated in the wings of the absorption, rather than at absorption peaks. For example, in the 540-nm region the values of polarization ratios at 535 and 545 nm (the approximate peak positions in the absorption spectrum of Fig. 1) are considerably different from the values in the wings. By taking the values from Fig. 6 at 527.5 and 560.5 nm as the fully resolved values, we obtain the set of components and angles for the two BPheo Q_x transition moments shown in Table 1. These components can be used to obtain the following set of angles between the two BPheo Q_x transition dipole moment vectors: 19 ± 5°, 63 ± 2°, 72 ± 2°, and 79 ± 2°.

None of these values compares well with the angle of 89 ± 1° obtained by Clayton and coworkers (15) from linear dichroism at the absorption maxima of reaction centers oriented in stretched films. By taking the data from Table 1 at the absorption maxima, we obtain the following set of angles between the BPheo Q_x transition moments: ≤16°, 55 ± 2°, 69 ± 2°, and 86 ± 2°. The last of these agrees reasonably well with the data from Clayton's laboratory, but we favor the use of data in the wings of the absorption spectrum. When high-resolution data becomes available in the 700–900 nm region more detailed comparisons should be possible to test the self-consistency of both approaches.

The polarization ratio data around 600 nm in Fig. 6 for the BChl Q_x bands provide evidence for at least three overlapping transitions. As in the 540-nm region, the polarization ratios change dramatically with λ beyond the main absorption band, particularly on the long-wavelength side in this case. A striking feature on this side is that P_1 is very low and nearly constant from 620 to 660 nm, whereas P_2 and P_3 change substantially, crossing each other. A simple explanation for this result can be offered based on the polarized photobleaching data of Rafferty and Clayton (16). These authors observe two pairs of photobleachable transitions, one at 600 nm (strong) and 630 nm (weak) and another at 810 nm (weak) and 870 nm (strong), which are interpreted as the two exciton components of the dimeric trap for the Q_x and Q_y transitions, respectively. If this is the case, one expects that the long-wavelength side of the polarization ratio data for the 600-nm band should originate primarily from the trap.

The small, constant magnitude of P_1 from 610 to 660 nm

Table 1. Polarization ratios (P_i), components (r_i), and angles (ϕ_i) for the Q_x transitions of BPheos in R-26 reaction centers determined at peaks and in the wings of the absorption band

λ, nm	i	P_i	r_i	ϕ_i
527.5 ± 0.3	1	+0.22 ± 0.03	0.46 ± 0.02	47 (133) ± 1°
	2	+0.12 ± 0.03	0.40 ± 0.02	51 (129) ± 1°
	3	−0.41 ± 0.05	0.14 ± 0.03	68 (112) ± 2°
535.0 ± 0.3	1	+0.22 ± 0.03	0.46 ± 0.02	47 (133) ± 1°
	2	+0.06 ± 0.03	0.37 ± 0.02	53 (127) ± 1°
	3	−0.33 ± 0.05	0.18 ± 0.03	65 (115) ± 2°
546.0 ± 0.3	1	+0.23 ± 0.03	0.47 ± 0.02	47 (133) ± 1°
	2	−0.10 ± 0.03	0.28 ± 0.01	58 (122) ± 1°
	3	−0.16 ± 0.05	0.25 ± 0.03	60 (120 ± 2°
560.5 ± 0.3	1	−0.04 ± 0.03	0.31 ± 0.02	56 (124) ± 1°
	2	−0.15 ± 0.03	0.26 ± 0.01	59 (121) ± 1°
	3	+0.17 ± 0.05	0.43 ± 0.03	49 (131) ± 2°

The P_i are corrected by using Eqs. 9 and 10 and the r_i are calculated from Eq. 4 with $k = 0.19 \pm 0.1$. Error limits represent 90% confidence intervals based on propagation of error in k and P_i (Fig. 6). $\phi_i = \cos^{-1}(\pm r_i^{1/2})$, so the experiment does not distinguish the angle from its complement, given in parentheses.

indicates that the component of the transition moment for each of the Q_x exciton transitions along magnetic axis 1 is the same and very small. Let us assume that peak 1 in the triplet ESR spectrum is associated with the averaged out-of-plane monomer z magnetic axes (these axes are uniquely defined for the nearly planar monomers). Then the data suggests that the monomer Q_x axes which combine to give symmetric and antisymmetric exciton components must be nearly perpendicular to the trap magnetic z axis. This does not necessarily require that the monomer z axes are parallel to each other, but it greatly restricts the set of possible pair geometries. If P_1 is found to be small and constant in the vicinity of the Q_y exciton bands, the analogous argument could also be made for the Q_y transitions and would require a plane parallel structure for $(BChl)_2$, a feature contained in both current models of the dimeric trap (34, 35).

The changes in P_2 and P_3 in the 600- to 660-nm range are also consistent with this analysis. By using polarized broadband irradiation ($850 < \lambda < 1200$ nm), we find that most (>70%) of the 870-nm transition moment lies along axis 2 (22). The polarized photobleaching data suggest that the 600-nm Q_x exciton component is roughly perpendicular to the 870-nm transition, whereas the weak 630-nm band is approximately parallel. Given the finding that the 870-nm transition is predominantly aligned along magnetic axis 2, the decrease in P_3 and increase in P_2 from 615 to 650 nm are explained by a shift from a transition perpendicular to 870 to one that is parallel to 870. This interpretation can be tested directly by tuning from 800 to 900 nm, where the trends for P_2 and P_3 are predicted to be the same for the Q_y transition.

In conclusion, the data presented here demonstrate that high-resolution magnetophotoselection can be applied successfully to the complex ordered array of chromophores in reaction centers. In addition to specifying the angular relationship between reaction center chromophores and the trap, we are encouraged that these experiments can provide direct insight into the relationship between the optical and averaged magnetic axes of the dimeric trap itself. This information then provides the basis for a more specific target for synthesis of artificial reaction centers (36–38). It should be noted that photoselection experiments do not reveal the angles between the intermolecular vectors joining the trap and other chromophores or the distances between components. In addition, experiments of this type provide only the orientation of vectors with respect to axes without specifying molecular structure. This is because the exact relationships between the transition dipole moments or magnetic axes and molecular structure remain unknown, though the subject of extensive theoretical investigations (39, 40). This problem can be resolved by spectroscopic analysis of the chromophore incorporated in a suitably oriented host crystal. Towards this end we have incorporated chlorophylls in the place of heme in apomyoglobin (41).

We thank Pam Axelson for expert preparation of reaction centers. R-26 cultures were generous gifts from Professors Clayton, Feher, and Sauer. We are grateful to Professor Brauman for parts of the dye laser and to Chris Chidsey for helpful discussions. This work was supported by National Science Foundation Grant CH7802070, by the Science and Education Administration of the U.S. Department of Agriculture under Grant 5901-0410-8-0147-0, and by the Stanford Institute for Energy Studies. M.G.R. is an International Business Machines Predoctoral Fellow. S.G.B. is a Fellow of the Alfred P. Sloan Foundation.

1. Clayton, R. K. & Wang, R. T. (1971) *Methods Enzymol.* **23**, 696–704.
2. Feher, G. & Okamura, M. Y. (1978) in *The Photosynthetic Bacteria*, eds. Clayton, R. K. & Sistrom, W. R. (Plenum, New York), pp. 349–386.
3. Norris, J. R., Uphaus, R. A., Crespi, H. L. & Katz, J. J. (1971) *Proc. Nat. Acad. Sci. USA* **68**, 625–628.
4. Feher, G., Hoff, A. J., Isaacson, R. A. & Ackerson, L. C. (1975) *Ann. N.Y. Acad. Sci.* **244**, 239–259.
5. Wraight, C. A. & Clayton, R. K. (1973) *Biochim. Biophys. Acta* **333**, 246–260.
6. Fajer, J., Brune, D. C., Davis, M. S., Forman, A. & Spaulding, L. D. (1975) *Proc. Natl. Acad. Sci. USA* **72**, 4956–4960.
7. Rockley, M. G., Windsor, M. W., Cogdell, R. J. & Parson, W. W. (1975) *Proc. Natl. Acad. Sci. USA* **72**, 2251–2255.
8. Kaufmann, K. J., Dutton, P. L., Netzel, T. L., Leigh, J. S. & Rentzepis, P. M. (1975) *Science* **188**, 1301–1304.
9. Moskowitz, E. & Malley, M. M. (1978) *Photochem. Photobiol.* **27**, 55–59.
10. Werner, H., Schulten, K. & Weller, A. (1978) *Biochim. Biophys. Acta* **502**, 255–268.
11. Parson, W. W., Clayton, R. K. & Cogdell, R. J. (1975) *Biochim. Biophys. Acta* **387**, 265–278.
12. Dutton, P. L., Leigh, J. S. & Reed, D. W. (1973) *Biochim. Biophys. Acta* **292**, 654–664.
13. Thurnauer, M. C., Katz, J. J. & Norris, J. R. (1975) *Proc. Natl. Acad. Sci. USA* **72**, 3270–3274.
14. Levanon, H. & Norris, J. R. (1978) *Chem. Rev.* **78**, 185–198.
15. Clayton, R. K., Rafferty, C. N. & Vermeglio, A. (1979) *Biochim. Biophys. Acta* **545**, 58–68.
16. Rafferty, C. N. & Clayton, R. K. (1979) *Biochim. Biophys. Acta* **545**, 106–121.
17. Rafferty, C. N. & Clayton, R. K. (1978) *Biochim. Biophys. Acta* **502**, 51–60.
18. Rafferty, C. N. & Clayton, R. K. (1979) *Biochim. Biophys. Acta* **546**, 189–206.
19. Vermeglio, A., Breton, J., Paillotin, G. & Cogdell, R. (1978) *Biochim. Biophys. Acta* **501**, 514–530.
20. Shuvalov, V. A. & Asadov, A. A. (1979) *Biochim. Biophys. Acta* **545**, 296–308.
21. Thurnauer, M. C. & Norris, J. R. (1977) *Chem. Phys. Lett.* **47**, 100–105.
22. Thurnauer, M. C. & Norris, J. R. (1976) *Biochem. Biophys. Res. Commun.* **73**, 501–506.
23. Sauer, K. (1975) in *Bioenergetics of Photosynthesis*, ed. Govindjee (Academic, New York), pp. 115–181.
24. Wasserman, E., Snyder, L. C. & Yager, W. A. (1964) *J. Chem. Phys.* **41**, 1763–1772.
25. Kottis, P. & Lefebvre, R. (1964) *J. Chem. Phys.* **41**, 379–393.
26. Goncalves, A. M. P. & Spendel, W. U. (1978) *Chem. Phys. Lett.* **54**, 611–615.
27. Kottis, P. & Lefebvre, R. (1964) *J. Chem. Phys.* **41**, 3660–3661.
28. Lhoste, J., Haug, A. & Ptak, M. (1966) *J. Chem. Phys.* **44**, 648–657.
29. El-Sayed, M. A. & Siegel, S. (1966) *J. Chem. Phys.* **44**, 1416–1423.
30. Siegel, S. & Judeikis, H. S. (1966) *J. Phys. Chem.* **70**, 2205–2211.
31. Judeikis, H. S. & Siegel, S. (1970) *J. Phys. Chem.* **74**, 1228–1235.
32. Frank, H. A., Bolt, J., Friesner, R. & Sauer, K. (1979) *Biochim. Biophys. Acta*, in press.
33. Birks, J. B. (1970) in *Photophysics of Aromatic Molecules* (Wiley, London), pp. 4–10 and 71.
34. Fong, F. K. (1975) *J. Am. Chem. Soc.* **97**, 6888–6892.
35. Boxer, S. G. & Closs, G. L. (1976) *J. Am. Chem. Soc.* **98**, 5406–5408.
36. Boxer, S. G. & Bucks, R. R. (1979) *J. Am. Chem. Soc.* **101**, 1883–1885.
37. Pellin, M. J., Kaufmann, K. J. & Wasielewski, M. R. (1979) *Nature (London)* **278**, 54–55.
38. Boxer, S. G. & Bucks, R. R., *Nature (London)*, in press.
39. Weiss, C. (1972) *J. Mol. Spectrosc.* **44**, 37–80.
40. Petke, J. D., Maggiora, G. M., Shipman, L. L. & Christoffersen, R. E. (1979) *Photochem. Photobiol.* **30**, 203–224.
41. Boxer, S. G. & Wright, K. A. (1979) *J. Am. Chem. Soc.*, in press.